# Mass-Transport and Heterogeneous Electron-Transfer Kinetics Associated with the Ferrocene/Ferrocenium Process in Ionic Liquids

*Cameron L. Bentley, Jiezhen Li, Alan M. Bond* and Jie Zhang**

School of Chemistry and Australian Research Council Centre of Excellence for Electromaterials Science, Monash University, Clayton, Vic 3800, Australia

**Abstract.** The ferrocene/ferrocenium ($Fc^{0/+}$) redox couple is regarded as a kinetically-facile process under voltammetric conditions. It also possesses a nearly "solvent independent" formal potential, and for this reason is commonly used as a "reference" redox system in electrochemical studies in non-aqueous electrolyte media. $Fc^{0/+}$ has also been adopted as a "model system" in ionic liquid (IL) media, although conflicting reports on the mass-transport and kinetics have brought its "ideality" into question. In this study, the mass-transport and heterogeneous electron-transfer kinetics associated with the $Fc^{0/+}$ process at a platinum electrode are reported in 14 ILs with dynamic viscosities ($\eta$) ranging from 20 to 620 cP. The diffusivity of Fc ($D_{Fc}$) was calculated in each of the ILs using convolution voltammetry and was found to be inversely proportional to the viscosity of the medium, as per the Stokes-Einstein relation (*i.e.*, $D \propto 1/\eta$). The heterogeneous electron-transfer rate constant ($k^0$) associated with the $Fc^{0/+}$ process was measured in each of the ILs using large-amplitude Fourier transformed alternating current (FTAC) voltammetry, and a plot of $\ln(k^0)$ vs. $\ln(\eta)$ was found to be linear, with a slope of -1.0, as predicted by the Marcus theory of electron transfer for an adiabatic process that involves predominantly solvent reorganization rather than inner-shell vibrations. Analysis of the $\ln(k^0)$ vs. $\ln(\eta)$ data suggests a slight dependence of $k^0$ on the constituent anion of the IL, which is thought to arise due to electrostatic interactions between the anion and positively charged $Fc^+$. Finally, extrapolating the $D$ vs. $1/\eta$ and $\ln(k^0)$ vs. $\ln(\eta)$ plots to $\eta$ values typically encountered in acetonitrile-based electrolyte media (*i.e.*, 0.5 cP) predicts $D$ and $k^0$ values of approximately $2 \times 10^{-5}$ cm$^2$ s$^{-1}$ and 10 cm s$^{-1}$, in excellent agreement with literature reports. Overall, the results presented in this study strongly suggest that the $Fc^{0/+}$ redox couple displays the characteristics of an "ideal" outer-sphere electron transfer process in IL media.

# Introduction

Electron transfer via homogeneous (*e.g.*, in solution) or heterogeneous (*e.g.*, across a phase boundary) processes are of considerable importance in both fundamental and applied chemistry. In the case of a heterogeneous process, where, for example, electron transfer occurs across an electrode/electrolyte interface, the rate of charge transfer (measured by the current flowing) is often governed by either the potential-dependent kinetics of the oxidation/reduction reaction or the mass-transport rate of electroactive species to/from the electrode surface (*e.g.*, diffusion). The kinetics and mechanisms of electron transfer and rate of mass-transport are usually strongly dependent upon the chemical (*i.e.*, electron donor/acceptor properties) and/or physical properties (*i.e.*, macroscopic viscosity) of the electrolyte media.[1-4]

Since their conception over two decades ago, air/water stable non-haloaluminate room temperature ionic liquids (ILs) have attracted significant interest in research and industry as replacements for volatile organic compounds (VOCs) in a range of applications.[5] Due to their intrinsic ionic conductivity and often high (electro)chemical stability, ILs have been employed extensively as electrolytes in electrochemical applications.[6] In addition, ILs have been referred to as 'designer solvents', referring to the fact that their physicochemical properties (*e.g.*, viscosity, Lewis acidity/basicity, hydrophobicity/hydrophilicity) can be 'tuned' to an extent by changing their constituent cation and/or anion.[6-7] It is these properties that make ILs ideal media for the study of the fundamentals of heterogeneous electron transfer, since, for example, the viscosity ($\eta$) and/or donor/acceptor properties of the medium can be varied systematically through simply changing cation and/or anion, all the while retaining relatively high ionic conductivity.[8] The latter point is particularly pertinent to the measurement of fast electron-transfer kinetics, where the main source of error is often uncompensated ohmic or $IR_u$ (where $R_u$ is uncompensated resistance) drop, particularly in analysis methods based on DC cyclic voltammetry.[2, 9]

Ferrocene (Fc) or bis($\eta^5$-cyclopentadienyl)iron is a common metallocene compound that undergoes a chemically reversible one-electron oxidation to ferrocenium ($Fc^+$), as shown in Eq. 1.

$$Fc \rightleftharpoons Fc^+ + e^- \quad \textbf{(1)}$$

The $Fc^{0/+}$ electron transfer reaction is a rapid, mechanistically simple, outer-sphere process.[1, 10] It also possesses a nearly "solvent independent" formal potential[11-12], and for this reason is commonly used as a "reference" redox process in non-aqueous electrolyte media.[13] In addition, since Fc and $Fc^+$ are uncharged and monocationic species, respectively, they should be relatively insensitive to ion-pairing effects and the structure of the electrical double layer (*i.e.*, double layer effects).[1, 3] Nonetheless, despite its status as a simple "model" redox process, the electrochemical characteristics of the $Fc^{0/+}$ process have remained controversial, with, for example, the reported[14] heterogeneous electron-transfer rate constant ($k^0$) of this process in acetonitrile (at platinum) ranging from ~0.01 to >100 cm $s^{-1}$.

Although the $Fc^{0/+}$ process has been investigated to a much lesser extent in IL media[15-21], similar controversies exist to those found in studies using molecular solvents. For example, some research groups have reported that $Fc^{0/+}$ displays the characteristics of an ideal, reversible (*i.e.*, mass-transport controlled) process under DC cyclic voltammetric conditions at moderate scan rates (*i.e.*, < 1 V $s^{-1}$), while others report quasi-reversible behaviour under the same, or similar conditions. Some of the widely different reported values of $k^0$ for the $Fc^{0/+}$ process in 1-ethyl-3-methylimidazolium bis(trifluoromethanesulfonyl)imide ($[C_2mim][NTf_2]$) are summarized in Table 1. In addition, the adherence of the diffusivity ($D$) of $Fc/Fc^+$ to the classical Stokes-Einstein relation[22] has also caused controversy, with early reports[15-16, 23] suggesting that $D_{Fc}$ is concentration dependent, while later reports[18, 21] have shown the predicted concentration-independent $D \propto 1/\eta$ behaviour.

**Table 1.** Reported $k^0$ values for the $Fc^{0/+}$ process at a platinum electrode in 1-ethyl-3-methylimidazolium bis(trifluoromethanesulfonyl)imide.

| $k^0$ (cm $s^{-1}$) | $T$ (K) | Technique | Reference |
|---|---|---|---|
| 0.0075 | 298 | DC Cyclic Voltammetry + Simulation | [24] |
| 0.010 ± 0.002 | 298 | Electrochemical Impedance Spectroscopy | [25] |
| 0.015 ± 0.008 | 298 | Electrochemical Impedance Spectroscopy | [19] |
| 0.021 ± 0.003 | 298 | DC Cyclic Voltammetry | [25] |
| 0.078 ± 0.014 | 298 | Scanning Electrochemical Microscopy | [20] |
| 0.15 – 0.20 | 293 | DC Cyclic Voltammetry | [26] |
| ≥0.18 | 303 | Electrochemical Impedance Spectroscopy | [21] |
| 0.21 ± 0.06 | 296 | High Speed Channel Electrode | [17] |

It is our goal to address these controversies in this study, by investigating the mass-transport and heterogeneous electron-transfer kinetics associated with the $Fc^{0/+}$ process in 14 ILs (structures shown in Scheme 1). As highlighted in a previous study[27], $D_{Fc}$ and $k^0$ ($Fc^{0/+}$) were measured using convolution voltammetry[28] and kinetically sensitive large-amplitude Fourier-transformed alternating current (FTAC) voltammetry[29-30], respectively. The trends in $D$ and $k^0$ have been related to the fluidity ($1/\eta$) of the pertinent ILs as per the predictions of classical Stokes-Einstein[22] and Marcus[1, 3] theories, respectively.

**Scheme 1.** Names, abbreviations and structures of the constituent cation/anions of the ILs used in this study.

| Cations | Anions |
|---|---|
| 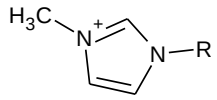 | 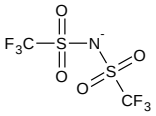 |
| 1-alkyl-3-methylimidazolium $[C_xmim]^+$ | bis(trifluoromethanesulfonyl)imide $[NTf_2]^-$ |
| 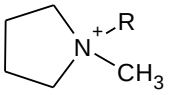 | 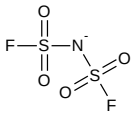 |
| 1-alkyl-1-methylpyrrolidinium $[C_xmpyr]^+$ | bis(fluorosulfonyl)imide $[FSI]^-$ |
| 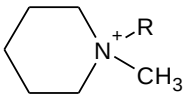 | 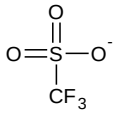 |
| 1-alkyl-1-piperidinium $[C_xmpip]^+$ | trifluoromethanesulfonate $[OTf]^-$ |
| 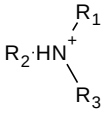 | 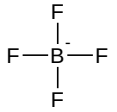 |
| trialkylammonium $[N_{H,x,y,z}]^+$ | tetrafluoroborate $[BF_4]^-$ |
| 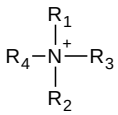 | 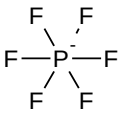 |
| tetraalkylammonium $[N_{w,x,y,z}]^+$ | hexafluorophosphate $[PF_6]^-$ |
| 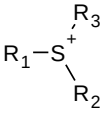 | 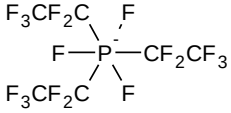 |
| trialkylsulfonium $[S_{x,y,z}]^+$ | tris(perfluoroalkyl)trifluorophosphate $[FAP]^-$ |

## Experimental

*Reagents.* 1-ethyl-3-methylimidazolium bis(trifluoromethanesulfonyl)imide ($[C_2mim][NTf_2]$, Io-li-tec), 1-butyl-3-methylimidazolium bis(trifluoromethanesulfonyl)imide ($[C_4mim][NTf_2]$, Io-li-tec), triethylsulfonium bis(trifluoromethanesulfonyl)imide ($[S_{2,2,2}][NTf_2]$, Solvent Innovation), ethyldimethylpropylammonium bis(trifluoromethanesulfonyl)imide ($[N_{1,1,2,3}][NTf_2]$, Merck), 1-butyl-1-methylpyrrolidinium bis(trifluoromethanesulfonyl)imide ($[C_4mpyr][NTf_2]$, Merck), 1-butyl-1-methylpyrrolidinium bis(fluorosulfonyl)imide ($[C_4mpyr][FSI]$, Boulder Ionics), 1-ethyl-3-methylimidazolium tris(perfluoroalkyl)trifluorophosphate ($[C_2mim][FAP]$, Merck), 1-ethyl-3-methylimidazolium trifluoromethanesulfonate ($[C_2mim][OTf]$, Solvent Innovation), 1-butyl-3-methylimidazolium tetrafluoroborate ($[C_4mim][BF_4]$, Solvent Innovation), 1-butyl-3-methylimidazolium hexafluorophosphate ($[C_4mim][PF_6]$, Io-li-tec), 1-butyl-1-methylpiperidinium bis(trifluoromethanesulfonyl)imide ($[C_4mpip][NTf_2]$, Io-li-tec), potassium ferricyanide ($K_3[Fe(CN)_6]$, Sigma-Aldrich) and potassium chloride (KCl, Merck) were used as received from the manufacturer. Ferrocene (Fc, Sigma-Aldrich, ≥ 98 %) was recrystallized from *n*-pentane (Merck, EMSURE) prior to use.

1-ethyl-3-methylimidazolium bis(fluorosulfonyl)imide ($[C_2mim][FSI]$) was prepared by a metathesis reaction between potassium bis(fluorosulfonyl)imide (K[FSI], Dai-ichi Kogyo Seiyaku Co., Ltd.) and 1-ethyl-3-methylimidazolium chloride ($[C_2mim]Cl$, Merck) in de-ionized water (Millipore Milli-Q Plus 185). Triethylammonium bis(trifluoromethanesulfonyl)imide ($[N_{H,2,2,2}][NTf_2]$) was prepared by a metathesis reaction between lithium bis(trifluoromethanesulfonyl)imide ($Li[NTf_2]$, 3M *Fluorad*) and triethylammonium chloride ($[N_{H,2,2,2}]Cl$, Sigma-Aldrich, recrystallized from ethanol) in de-ionized water. Tributylmethylammonium bis(trifluoromethanesulfonyl)imide ($[N_{1,4,4,4}][NTf_2]$) was prepared by a metathesis reaction between $Li[NTf_2]$ and tributylmethylammonium

methylsulfate ([$N_{1,4,4,4}$][$CH_3OSO_3$], Sigma-Aldrich) in de-ionized water. Following synthesis, the ILs were taken up in dichloromethane (EMSURE, Merck) and rinsed repeatedly with de-ionized water to extract residual water soluble salt (i.e., KCl, LiCl or Li[$CH_3OSO_3$]). Before use, each of the ILs was dried under high vacuum ($\leq 10^{-1}$ mbar) at 45°C for 48 hours. The residual water content was less than 100 ppm by Karl Fischer titration (Metrohm 831 KF Coulometer). The viscosity of the neat ILs was measured measured using the falling ball method with an Anton Paar Automated Microviscometer (AMVn). Density was measured with an Anton Paar DMA 4500M Density Meter.

*Electrochemical instrumentation and procedures.* DC cyclic voltammetric experiments were carried out using a CHI 760E electrochemical workstation (CH Instruments, USA), while FTAC voltammetric experiments were undertaken with home built instrumentation.[30] In the FTAC voltammetric experiments, a sinusoidal waveform made up of either a single frequency, $f$, or dual frequencies[27], $f_1$ and $f_2$ (where $f_1$ and $f_2$ are the lower and higher frequencies, respectively), and amplitude ($\Delta E$) 160 mV, was superimposed onto a DC ramp with a scan rate, $\upsilon$. All voltammetric experiments were carried out at 22 ± 2°C using a standard 3-electrode arrangement with a platinum microdisk (nominal diameter = 50 μm) as the working electrode, the appropriate reference electrode (see below) and a Pt wire auxiliary electrode. The platinum microdisk was fabricated in-house by heat sealing a 0.05 mm diameter microwire (annealed, 99.99%, Goodfellow, UK) in a borosilicate glass capillary under vacuum, as reported elsewhere.[31] The quasi-reference electrode in IL media was a Pt wire and the reference electrode in aqueous media was Ag/AgCl (3 M NaCl). The quasi-reference electrode potential was calibrated against the recommended $Fc^{0/+}$ process. Prior to voltammetric experimentation, the Pt microdisk electrode was activated by polishing with successively smaller (1, 0.3 and 0.05 μm) aqueous alumina slurries (Kemet, UK) on clean polishing cloths (Buehler, USA), followed by thorough rinsing with de-ionized water and then acetone. The electrochemically

active area ($A$) of the Pt microdisk was calibrated with convolution voltammetry[28, 32], using the reduction of a $[Fe(CN)_6]^{3-}$ solution of known concentration (4.0 mM in aqueous media containing 1.0 M KCl) and adopting a diffusion coefficient of $7.6 \times 10^{-6}$ cm$^2$ s$^{-1}$, as published under these conditions.[33]

*Simulations and data analysis.* DC cyclic voltammetric simulations were carried out using the commercially available DigiElch digital simulation software (v. 7F, Elchsoft, Germany). Inlaid disk electrode geometry ($r_0$ = 0.0025 cm) was assumed in DC cyclic voltammetric simulations and the contribution from two-dimensional (radial) diffusion to mass-transport was considered.

FTAC voltammetric simulations were carried out with the Monash Electrochemistry Simulator (MECSim) software package (http://www.garethkennedy.net/MECSim.html). This Fortran software uses the expanding spatial grid formulation[34] and is based on the mathematical approach derived by Rudolph[35] with minor variations to solve one-dimensional linear diffusion problems. Simulations of the electrode kinetics were based on Butler-Volmer theory[1] and the use of electron transfer reaction shown in Eq. 2.

$$A \rightleftharpoons A^+ + e^-; (E^0, k^0, \alpha) \quad \textbf{(2)}$$

where $E^0$ *is* the reversible potential, $k^0$ is the heterogeneous electron-transfer rate constant and $\alpha$ is the charge transfer coefficient. Planar electrode geometry ($A$ = $1.96 \times 10^{-5}$ cm$^2$) was assumed in FTAC voltammetric simulations and only the contribution from one-dimensional (planar) diffusion to mass-transport was considered. FTAC voltammetric data obtained from either experiment or simulation in the time domain were converted to the frequency domain to generate the power spectrum. AC harmonics and the corresponding aperiodic DC component were selected from the power spectrum. Band filtering and inverse Fourier transform was then

used to obtain the required resolved DC and AC components as a function of either time or potential.[36-37]

The AC frequencies ($f$ or $f_1$ and $f_2$), AC amplitude ($\Delta E$), scan rate ($\upsilon$) and temperature ($T$) were assumed to be accurately known and uncompensated resistance ($R_u$), the electrode area ($A$), $E^0$, bulk concentration ($C^b$), diffusion coefficient ($D$) and double layer capacitance ($C_{dl}$) were measured experimentally, prior to quantifying $k^0$. For the near-reversible $Fc^{0/+}$ process, the simulated data were found to be relatively insensitive to $\alpha$ in the range $0.5 \pm 0.1$, so its value was assumed to be equal to 0.50 in all simulations. $R_u$ was estimated in a potential region where no faradaic process occurs by electrochemical impedance spectroscopy (amplitude = 5 mV, frequency range = 100 Hz to 100 kHz) by fitting the data with an RC equivalent circuit. Since $Fc^{0/+}$ was the process under investigation, $E^0$ was defined as 0 V (vs. $Fc^{0/+}$) in all simulations. $C^b$ was calculated based on the known mass of the electroactive species and volume of the solution. $D_{Fc}$ was estimated from DC cyclic voltammetric data using convolution, as described elsewhere.[28] As only the contribution from linear (planar) diffusion to mass-transport was considered in the theory (see above), the simulated data was found to be insensitive to $D_{Fc^+}$. Therefore, despite the fact that $D_{Fc^+}$ is known to be markedly different from $D_{Fc}$ in some ILs[18], in all FTAC voltammetric simulations it was assumed that $D_{Fc^+} = D_{Fc}$. $C_{dl}$ was quantified from the background current in the fundamental harmonic of the $f_2$ dataset, at potentials where AC faradaic current is absent. In order to define the potential dependence of $C_{dl}$, a non-linear capacitor model was used, as described elsewhere[38]:

$$C_{dl}(t) = C_0 + C_1E(t) + C_2E^2(t) + C_3E^3(t) + C_4E^4(t) \quad \textbf{(3)}$$

Finally, using the assumption that $\alpha$ is 0.50, $k^0$ was determined by comparison of experimental and simulated higher order AC harmonics, as described in the Results and Discussion sections of the main text.

## Results

**Measurement of *D* with Convolution Voltammetry.** The $Fc^{0/+}$ process was initially characterized in a range of ILs using DC cyclic voltammetry at a Pt microdisk electrode; a representative cyclic voltammogram obtained in $[C_2mim][NTf_2]$ is shown in Figure 1a. The cyclic voltammogram displays characteristics intermediate between those expected for the 'steady-state' and 'transient' regimes, indicating that the contribution from both radial and planar diffusion to mass-transport is significant under the investigated conditions.[28] The diffusivity of Fc and $Fc^+$ were estimated to be $3.9 \times 10^{-7}$ and $3.3 \times 10^{-7}$ $cm^2$ $s^{-1}$, respectively, through simulation-experimental comparison (also shown in Figure 1a). The difference between $D_{Fc}$ and $D_{Fc^+}$ is consistent with the results by Compton and co-workers[18], who studied the $D_{Fc}/D_{Fc^+}$ ratio in a range of ILs. In addition, the simulated data also indicates that the $Fc^{0/+}$ process is electrochemically reversible under the conditions relevant to Figure 1, which is consistent with some literature reports.[17, 21]

In order to quantify the diffusivity of Fc without resorting to simulation-experiment comparisons, the forward sweep of the cyclic voltammograms ($I-E$ data) obtained in each IL (example shown Figure 1a) were transformed using a convolutive technique[28]; an example of a convolved-current voltammogram ($M-E$ data) obtained using this technique is shown in Figure 1b. Clearly, the convolved-current voltammogram superficially resembles a steady-state voltammogram, with a sigmoidal-shape and a well-defined mass-transport limited current plateau. Under purely diffusion-controlled conditions, the convolved current ($M$) reaches its maximum or limiting value, $M_L$:

$$M_L = nAFC^b\sqrt{D} \qquad \textbf{(4)}$$

where $n$ is the stoichiometric number of electrons, A is the electrode area, $F$ is Faraday's constant and $C^b$ is the bulk concentration. By substituting the appropriate values into Eq. 4, the

diffusion coefficient of Fc was determined to be $3.9 \times 10^{-7}$ cm$^2$ s$^{-1}$ in [$C_2$mim][$NTf_2$], in agreement with the simulated data shown in Figure 1a. In addition, $M_L$ was found to scale linearly with $C_b$ in the range 3 to 15 mM, indicating that $D_{Fc}$ is independent of the bulk concentration of Fc, which is at odds with some literature reports[15-16, 23], but in agreement with others[18, 39-41] (explored below). The $D_{Fc}$ values calculated in each of the ILs using convolution voltammetry are summarized in Table 2.

**Table 2.** Summary of the $D_{Fc}$ values measured using convolution voltammetry in a range of ILs.

| IL | $\eta$ (cP)† | $D_{Fc}$ ($\times 10^7$ cm$^2$ s$^{-1}$) |
|---|---|---|
| [$C_2$mim][$NTf_2$] | 37.1 | 3.9 |
| [$S_{2,2,2}$][$NTf_2$] | 38.3 | 3.6 |
| [$C_4$mim][$NTf_2$] | 56.8 | 2.7 |
| [$N_{H,2,2,2}$][$NTf_2$] | 57.2 | 2.7 |
| [$N_{1,1,2,3}$][$NTf_2$] | 88.2 | 1.8 |
| [$C_4$mpyr][$NTf_2$] | 90.6 | 1.9 |
| [$C_4$mpip][$NTf_2$] | 223 | 0.83 |
| [$N_{1,4,4,4}$][$NTf_2$] | 618 | 0.32 |
| [$C_2$mim][FSI] | 21 | 6.5 |
| [$C_2$mim][OTf] | 55.6 | 2.6 |
| [$C_4$mpyr][FSI] | 58.9 | 2.8 |
| [$C_2$mim][FAP] | 70.2 | 2.4 |
| [$C_4$mim][$BF_4$] | 124 | 1.1 |
| [$C_4$mim][$PF_6$] | 294 | 0.53 |

†Viscosity of the neat IL at 22°C.

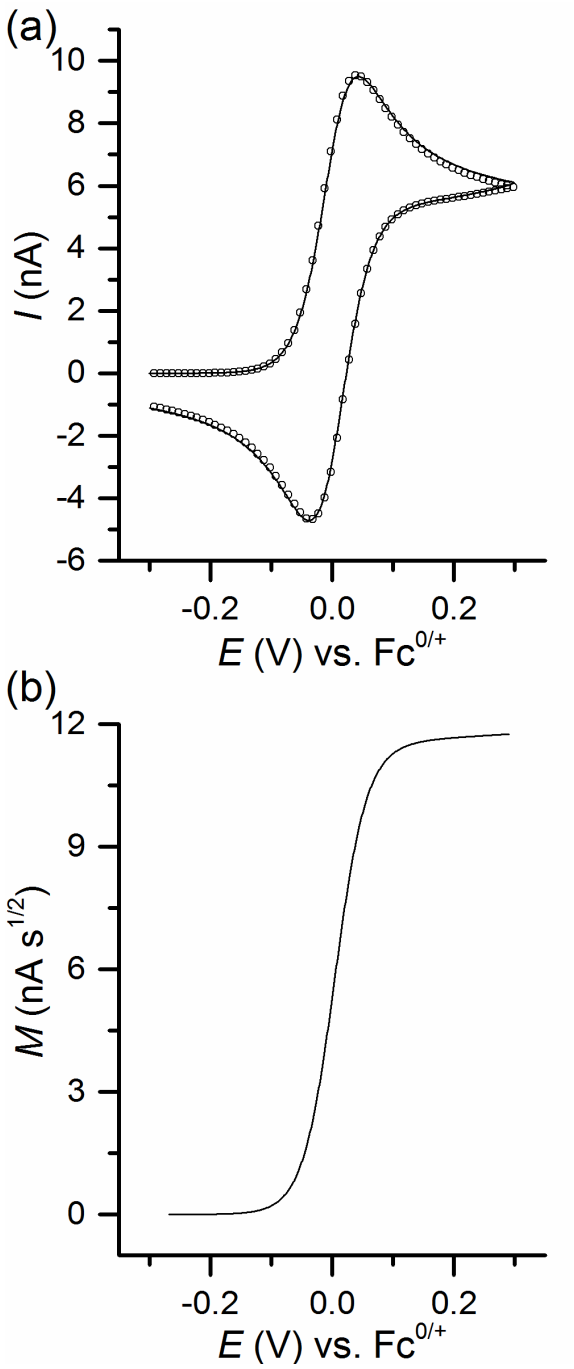


**Figure 1.** (a) Cyclic and (b) convolved-current voltammograms obtained from 9.6 mM Fc in [$C_2$mim][$NTf_2$] at a 50 µm diameter Pt microdisk electrode with a scan rate of 50 mV $s^{-1}$. Also included in (a) is simulated data (○) obtained for a reversible process with reversible potential ($E^0$) = 0 V, $D_{Fc}$ = 3.9 × $10^{-7}$ $cm^2$ $s^{-1}$, $D_{Fc^+}$ = 3.25 × $10^{-7}$ $cm^2$ $s^{-1}$, $R_u$ = 0 Ω and double layer capacitance ($C_{dl}$) = 0 F.

**Measurement of $k^0$ by FTAC Voltammetry.** The $Fc^{0/+}$ process generally possesses fast electrode kinetics[10], and, as previously alluded to, was found to be electrochemically reversible in all of the ILs under DC cyclic voltammetric conditions at a 50 μm diameter Pt microdisk with a scan rate of 50 mV $s^{-1}$. In order to quantify $k^0$ for the $Fc^{0/+}$ process, FTAC voltammetry was employed, in which a sinusoidal (or other periodic waveform) with amplitude, $\Delta E$, is superimposed onto the DC ramp for significant advantages, as detailed elsewhere.[29-30, 33] In a previous study[27], we outlined a dual-frequency designer waveform which can be used to reliably quantify the electrode kinetics of processes approaching the reversible limit. In this approach, two frequencies, a low 'reference' frequency ($f_1$) and a high 'detection' frequency ($f_2$) are applied simultaneously. The $f_1$ dataset, collected on a timescale where the target process is reversible, is used as an internal reference to calibrate $A$, $D$, $C$ and $R_u$, and these calibrated values are subsequently used to calculate $k^0$ from analysis of the $f_2$ dataset, where the target process is quasi-reversible.

The dual-frequency method was used to calculate the $k^0$ value associated with the $Fc^{0/+}$ process in all of the ILs except the three most viscous ones (see Table 3); representative dual-frequency FTAC voltammograms obtained in $[C_2mim][NTf_2]$ are shown in Figures 2 and 3. In the highly viscous ILs, the $Fc^{0/+}$ process was found to be far from reversible, even at frequencies as low as 9 Hz (explained below), and for this reason, the dual-frequency approach was not necessary; a representative single-frequency FTAC voltammogram obtained in tributylmethylammonium bis(trifluoromethanesulfonyl)imide ($[N_{1,4,4,4}][NTf_2]$) is shown in the Supporting Information, Figure S1.

The low frequency dataset ($f_1$ = 9 Hz, $f_2$ = 182 Hz, $\Delta E$ = 160 mV) obtained from the $Fc^{0/+}$ process in $[C_2mim][NTf_2]$ is shown in Figure 2. It should be noted that in the simulations, mass-transport was assumed to occur solely by planar (1D) diffusion (see the Experimental Section). This is a valid approximation, despite the micro-sized electrode geometry (50 μm

diameter), as the extremely low diffusion coefficients encountered in IL media (typically in the $10^{-8}$ to $10^{-7}$ $cm^2$ $s^{-1}$ range) result in an extremely contracted diffusion layer, making the contribution from radial (2D) diffusion on the AC timescale negligible. However, as noted above, under DC conditions, radial diffusion makes a significant contribution to mass-transport and for this reason the aperiodic DC data were not included in the theory-experiment comparison. There is generally excellent agreement between the simulated and experimental data up to at least the 7th harmonic in the low frequency ($f_1$) dataset. The $Fc^{0/+}$ process can be treated as reversible on this timescale, allowing the *A*, *D*, *C* and $R_u$ values to be calibrated, as highlighted above.

The high frequency ($f_1$ = 9 Hz, $f_2$ = 182 Hz, $\Delta E$ = 160 mV) dataset obtained from the $Fc^{0/+}$ process in $[C_2mim][NTf_2]$ is shown in Figure 3. As can be seen in the 9th and 10th harmonic components, the $Fc^{0/+}$ process can be treated as quasi-reversible on this timescale. Evidently, excellent agreement between the simulated and experimental data was achieved using the calibrated *A*, *D*, *C* and $R_u$ values and a $k^0$ value of 0.14 cm $s^{-1}$ ($\alpha$ was assumed to be 0.50, as noted in the Experimental Section). The determined $k^0$ value is in good agreement with that measured by Compton and co-workers[17], 0.21 ± 0.06 cm $s^{-1}$ (see Table 1) adding confidence to the quality of the collected data. Finally, in order to confirm that $R_u$ has been correctly accommodated for in the simulation, FTAC voltammetric data was collected at a 3-fold lower Fc concentration; the $f_1$ and $f_2$ datasets are shown in Figures S2 and S3, respectively. As expected, the determined $k^0$ value is independent of Fc concentration, with a value of 0.14 cm $s^{-1}$ also being measured from the low-concentration dataset, adding further confidence to the quality of the collected data.

The FTAC voltammogram ($f$ = 9 Hz, $\Delta E$ = 160 mV) obtained from the $Fc^{0/+}$ process in $[N_{1,4,4,4}][NTf_2]$ is shown in Figure S1. As can be seen from the 7th and 8th harmonic data, the $Fc^{0/+}$ process is far from reversible in this highly viscous IL ($\eta$ = 615 cP), even at this relatively

low frequency of 9 Hz. Excellent agreement between the simulated and experimental data was achieved using the measured *A*, *D*, *C* and $R_u$ values and a $k^0$ value of 0.007 cm $s^{-1}$. Evidently, the $k^0$ value measured in highly viscous $[N_{1,4,4,4}][NTf_2]$ is more than an order of magnitude lower than that measured in relatively fluid $[C_2mim][NTf_2]$, in qualitative agreement with what is predicted by Marcus theory (discussed below).[1, 3] Using this approach, or the dual-frequency approach outlined above, the heterogeneous electron transfer kinetics of the $Fc^{0/+}$ process was measured in each of the 14 different ILs outlined in the Experimental Section (see Scheme 1); the FTAC voltammetric data are included in the Supporting Information (see Figures S4 to S31) and the measured $k^0$ values are summarized in Table 3.

**Table 3.** Summary of the $k^0$ ($Fc^{0/+}$) values measured using FTAC voltammetry in a range of ILs.

| IL | $\eta$ (cP)[†] | $k^0$ (cm $s^{-1}$) |
|---|---|---|
| $[C_2mim][NTf_2]$ | 37.1 | 0.14 |
| $[S_{2,2,2}][NTf_2]$ | 38.3 | 0.13 |
| $[C_4mim][NTf_2]$ | 56.8 | 0.090 |
| $[N_{H,2,2,2}][NTf_2]$ | 57.2 | 0.095 |
| $[N_{1,1,2,3}][NTf_2]$ | 88.2 | 0.072 |
| $[C_4mpyr][NTf_2]$ | 90.6 | 0.065 |
| $[C_4mpip][NTf_2]$ | 223 | 0.023 |
| $[N_{1,4,4,4}][NTf_2]$ | 618 | 0.007 |
| $[C_2mim][FSI]$ | 21 | 0.21 |
| $[C_2mim][OTf]$ | 55.6 | 0.11 |
| $[C_4mpyr][FSI]$ | 58.9 | 0.10 |
| $[C_2mim][FAP]$ | 70.2 | 0.055 |
| $[C_4mim][BF_4]$ | 124 | 0.050 |
| $[C_4mim][PF_6]$ | 294 | 0.013 |

[†]Viscosity of the neat IL at 22°C.

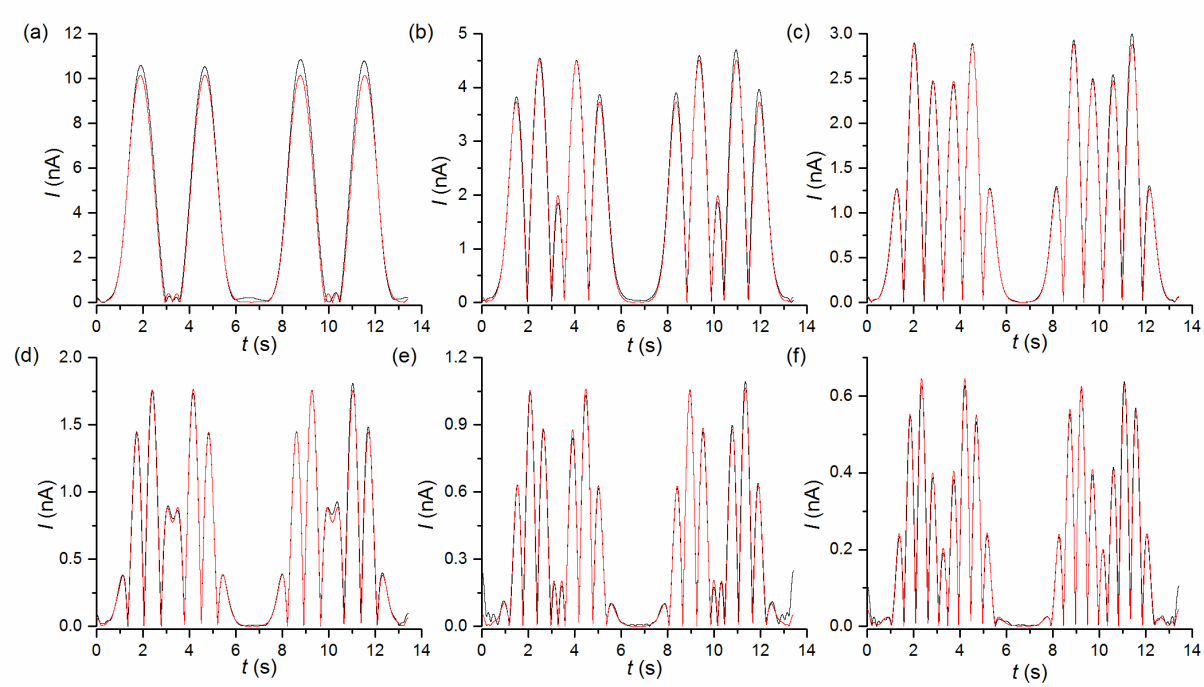


**Figure 2.** Comparison of the experimental (—) FTAC voltammograms obtained from 9.6 mM Fc in [$C_2$mim][$NTf_2$] with a 50 µm dia. Pt microdisk electrode at a (reference) frequency of 9 Hz and the simulated ones for a reversible one-electron transfer process (—). During the voltammetric perturbation, two frequencies, $f_1$ = 9 Hz and $f_2$ = 182 Hz, were applied simultaneously, superimposed on a DC linear ramp with a scan rate of 0.14901 V $s^{-1}$. (a) to (f) correspond to the 2$^{st}$ to 7$^{th}$ harmonics. The simulation parameters are: $A$ = 1.96 × $10^{-5}$ $cm^2$, $f_1$ = 9 Hz and $f_2$ = 182 Hz, $\Delta E$ = 160 mV, $D$ = 3.9 × $10^{-7}$ $cm^2$ $s^{-1}$, $R_u$ = 12 kΩ, $E^0$ = 0 V vs. $Fc^{0/+}$, $C_{dl}$ ($C_0$ = 7.8, $C_1$ = -1.3, $C_2$ = 2.5, $C_3$ = 1.6, $C_4$ = -2.8) µF $cm^{-2}$ (see Eq. 3) and $T$ = 296 K.

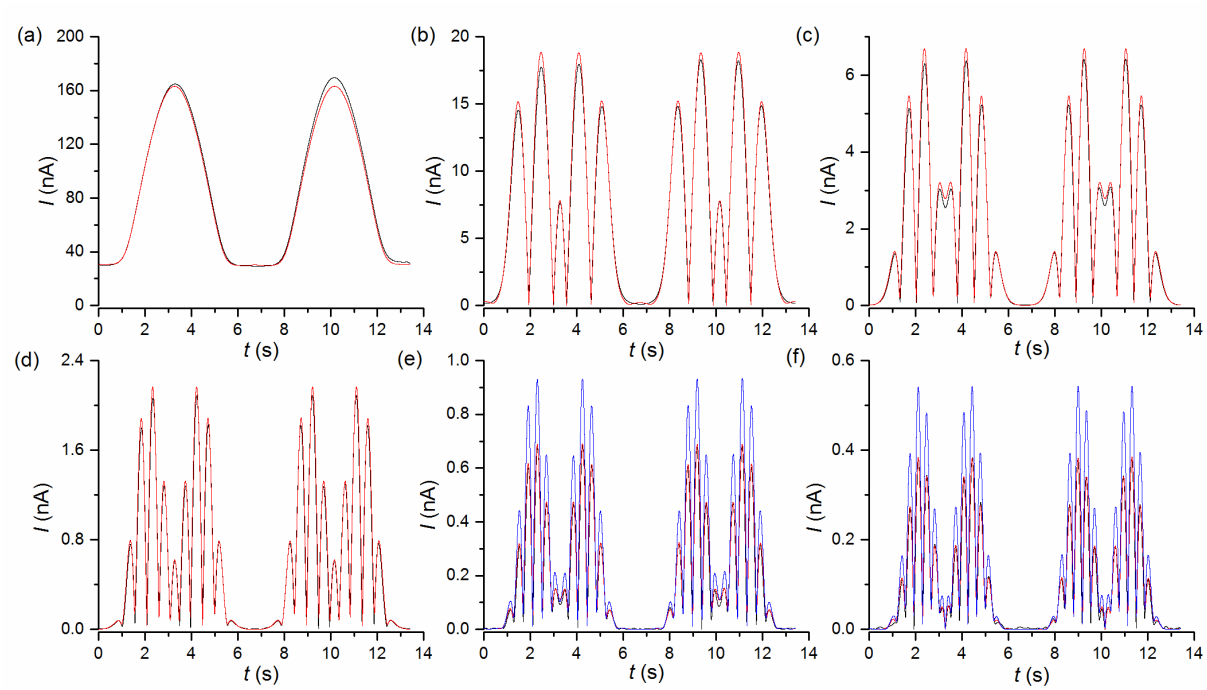


**Figure 3.** Comparison of the simulated (—) and experimental (—) FTAC voltammograms obtained from 9.6 mM Fc in $[C_2mim][NTf_2]$ with a 50 µm dia. Pt microdisk electrode at a (detection) frequency of 182 Hz. During the voltammetric perturbation, two frequencies, $f_1$ = 9 Hz and $f_2$ = 182 Hz, were applied simultaneously, superimposed on a DC linear ramp with a scan rate of 0.14901 V $s^{-1}$. (a) to (j) correspond to the 1st, 3rd, 5th, 7th, 9th and 10th harmonics. The simulation parameters are: $A = 1.96 \times 10^{-5}$ $cm^2$, $f_1$ = 9 Hz and $f_2$ = 182 Hz, $\Delta E$ = 160 mV, $D = 3.9 \times 10^{-7}$ $cm^2$ $s^{-1}$, $R_u$ = 12 kΩ, $k^0$ = 0.14 cm $s^{-1}$, $\alpha$ = 0.50, $E^0$ = 0 V vs. $Fc^{0/+}$, $C_{dl}$ ($C_0$ = 7.8, $C_1$ = -1.3, $C_2$ = 2.5, $C_3$ = 1.6, $C_4$ = -2.8) µF $cm^{-2}$ (see Eq. 3) and $T$ = 296 K. The 9th and 10th harmonic for a reversible case (—) are also shown for comparison in (e) and (f), respectively.

## Discussion

**Mass-Transport.** As shown in Eq. 5, the diffusion coefficient or diffusivity of a solute in solution is inversely proportional to the frictional force (or frictional drag) acting upon it.

$$D = \frac{k_{\mathrm{B}}T}{F_{\mathrm{d}}} \quad \textbf{(5)}$$

This is a form of the Einstein-relation, where $k_{\mathrm{B}}$ is the Boltzmann constant, $T$ is the absolute temperature and $F_{\mathrm{d}}$ is a friction coefficient.[22] If the dissolved solute is likened to a rigid solid sphere with a radius, $r_{\mathrm{H}}$, diffusing in a continuum of solvent with a viscosity, $\eta$, $F_{\mathrm{d}}$ can be calculated using Stokes-Law[42-43], which is shown in Eq. 6.

$$F_{\mathrm{d}} = 4\pi\eta r_{\mathrm{H}} + 2\pi\eta r_{\mathrm{H}} = 6\pi\eta r_{\mathrm{H}} \quad \textbf{(6)}$$

where the first term represents a force due to pressure built up in front of a diffusing solute and the second term is a frictional force parallel to its surface.[42, 44-45] Combining Eqs. 5 and 6 gives the Stokes-Einstein equation[22], shown in Eq. 7.

$$D = \frac{k_{\mathrm{B}}T}{6\pi\eta r_{\mathrm{H}}} \quad \textbf{(7)}$$

The Stokes-Einstein equation, as written in Eq. 7, is strictly only valid when the size of the solute is large compared to the size of the solvent (*i.e.*, when $r_{\mathrm{solute}}/r_{\mathrm{solvent}} > 5$). To accommodate this fact, the Stokes-Einstein equation is often written in the form shown in Eq. 8.

$$D = \frac{k_{\mathrm{B}}T}{c\pi\eta r_{\mathrm{H}}} \quad \textbf{(8)}$$

where $c$ is a constant with a value of 4 ('perfect slip') or 6 ('perfect stick').[42] The value of 4 arises because the second term of Eq. 6 (*i.e.*, from frictional force parallel to the solute surface) disappears when the solvent is able to 'slip past' the surface of a small solute particle.[42, 46] In

practice, an empirical constant with a value between 4 and 6 is often used for small solutes in conventional solvents[42, 44-45] and ionic liquids.[47-48]

In any case, if it is assumed that the constant, $c$, and Stokes radius, $r_H$, of Fc are IL-independent, a plot of $D$ vs. $1/\eta$ is predicted to be linear, as is shown in Figure 4a. Evidently, the $D$ vs. $1/\eta$ plot is linear ($r^2 = 0.99$) and passes through the origin, within experimental error. As previously alluded to in the Introduction Section, adherence to the Stokes-Einstein relation (*i.e.*, $D_{Fc} \propto 1/\eta$) in ILs is in agreement with previous work in our group on the mass-transport of protons[39] and cobaltocenium[40], as well as the work by Compton and co-workers on the mass-transport of ferrocene[18] and *N*,*N*,*N*',*N*'-tetramethyl-*p*-phenylenediamine[41], but is at odds with earlier work by a number of research groups.[15-16, 23] The value of $r_H$, calculated from the slope of the $D$ vs. $1/\eta$ curve (obtained by linear regression of the experimental data) with $c = 6$ is 1.7 Å and with $c = 4$ is 2.5 Å, in agreement with the work by Hussey and co-workers.[21] The Stokes radius calculated assuming $c = 4$ is in much closer agreement with the radius of ferrocene in the solid state, as measured by X-ray diffraction (2.7 Å).[49-50] This suggests that the mass-transport of ferrocene approaches 'perfect slip' behaviour in IL media (*i.e.*, $c = 4$), which is unsurprising, given that the constituent anions and cations of the ILs are comparable in size or larger than the Fc molecule (*e.g.*, the estimated ionic radii of $[BF_4]^-$, $[PF_6]^-$, $[OTf]^-$ and $[NTf_2]^-$ are 2.29, 2.54, 2.70 and 3.25 Å, respectively).[42] Finally, extrapolating the plot shown in Figure 4a to $\eta$ = 0.48 cP, which is the viscosity of an acetonitrile solution containing 0.3 M $[NBu_4][ClO_4]$ (where $[NBu_4]^+$ is the tetrabutylammonium cation) at 22°C, and assuming the constant in Eq. 8 is 6,[51] gives a $D_{Fc}$ value of approximately $2 \times 10^{-5}$ cm$^2$ s$^{-1}$, which is consistent with the value reported by Sun and Mirkin ($2.05 \times 10^{-5}$ cm$^2$ s$^{-1}$) under these conditions.[10]

**Electrode Kinetics.** In the Marcus Theory of electron transfer, the heterogeneous rate constant associated with a simple, outer sphere electron transfer (see Eqs. 1 and 2) is related to the standard free energy of activation, $\Delta G^{\ddagger}$, through the expression shown in Eq. 9.[1, 3]

$$k^0 = K_{\mathrm{P}} \nu_{\mathrm{n}} \kappa_{\mathrm{el}} \exp\left(-\frac{\Delta G^{\ddagger}}{RT}\right) \quad \textbf{(9)}$$

where $R$ is the gas constant, $K_{\mathrm{P}}$ is the precursor equilibrium constant, representing the ratio of the reactant concentration (*e.g.*, O or R in Eq. 2) in the reactive position (*i.e.*, precursor state) at the electrode to its bulk concentration; $\nu_{\mathrm{n}}$ is the nuclear frequency factor, representing the frequency of attempts on the energy barrier (*i.e.*, through bond vibrations or solvent motion); and $\kappa_{\mathrm{el}}$ is the electronic transmission coefficient, which is related to the probability of electron tunneling (*i.e.*, adiabaticity parameter). The total activation energy, $\Delta G^{\ddagger}$, can be separated into two components, the inner-shell ($\Delta G_{\mathrm{is}}^{\ddagger}$) and outer-shell ($\Delta G_{\mathrm{os}}^{\ddagger}$) activation energies. $\Delta G_{\mathrm{is}}^{\ddagger}$ is proportional to the inner-shell reorganization energy, $\lambda_{\mathrm{i}}$, which is related to changes in bond lengths (*i.e.*, reorganization of species O or R in Eq. 2) during electron transfer. $\Delta G_{\mathrm{os}}^{\ddagger}$ is proportional to the outer-shell reorganization energy, $\lambda_{\mathrm{o}}$, which is related to changes in solvation (*i.e.*, reorganization of the solvent) during electron transfer.

For an adiabatic electron transfer reaction that involves predominantly solvent reorganization rather than inner-shell vibrations (*i.e.*, $\Delta G_{\mathrm{is}}^{\ddagger} < \Delta G_{\mathrm{os}}^{\ddagger}$), Marcus theory predicts that $\nu_{\mathrm{n}}$ is proportional to the inverse of the longitudinal relaxation time of the solvent, $\tau_{\mathrm{L}}$, as is shown in Eq. 10.[1, 3, 52]

$$\nu_{\mathrm{n}} = \tau_{\mathrm{L}}^{-1} \left(\frac{\Delta G_{\mathrm{os}}^{\ddagger}}{4\pi RT}\right)^{1/2} \quad \textbf{(10)}$$

Thus, for a given electron transfer reaction (*i.e.*, $Fc^{0/+}$, see Eq. 1), if it is assumed that the pre-exponential factors $K_{\mathrm{P}}$ and $\kappa_{\mathrm{el}}$ are solvent independent, Eq. 9 can be rewritten as shown in Eq. 11.[3, 53]

$$k^0 = A_{\mathrm{P}} \tau_{\mathrm{L}}^{-\theta} \exp\left(-\frac{\Delta G^{\ddagger}}{RT}\right) \quad \textbf{(11)}$$

where $A_P$ is the portion of the pre-exponential factor which is approximated as being solvent independent and θ is a fraction between 0 and 1 that depends on the degree of reaction adiabacity and the relative magnitudes of $\Delta G_{is}^{\ddagger}$ and $\Delta G_{os}^{\ddagger}$ (*i.e.*, θ = 1 for a strongly adiabatic reaction where $\Delta G_{is}^{\ddagger} < \Delta G_{os}^{\ddagger}$). Consequently, a plot of ln($k^0$) vs. ln($\tau_L$) is expected to be linear, with a slope of –θ, as shown in Eq. 12.

$$\ln (k^0) = [\ln (\ A_P) - \frac{\Delta G^{\ddagger}}{RT}] - \theta \ln (\tau_L) \quad \textbf{(12)}$$

This phenomenon is known as the 'solvent dynamic effect' and its influence on the electron transfer rate of redox molecules whose activation free energy is dominated by the outer-shell component have been reported in a number of studies.[52-55]

$\tau_L$ is approximately proportional to the macroscopic viscosity of the solvent[53, 56-57], including in ILs[58-59], and, in theory can be calculated using Eq. 13.

$$\tau_L = 3V_m(\varepsilon_\infty/\varepsilon_0)\ \eta/RT \quad \textbf{(13)}$$

where $V_m$ is the molar volume of the medium and $\varepsilon_\infty$ and $\varepsilon_0$ are the high-frequency and static permittivities, respectively. Unfortunately, $\varepsilon_\infty$ and $\varepsilon_0$ values are not available for most of the ILs investigated in this study; however, by substituting Eq. 13 into Eq. 12, Eq. 14 can be derived.

$$\ln (k^0) = [l\ln (A_P) - \frac{\Delta G^{\ddagger}}{RT}] - \theta \ln (\frac{3V_m\varepsilon_\infty}{\varepsilon_0 RT}) - \theta \ln (\eta) \quad \textbf{(14)}$$

Therefore, if it is assumed that the first term is fixed for the $Fc^{0/+}$ couple (*i.e.*, $\Delta G^{\ddagger}$ is solvent independent), and the second term is relatively independent of the IL structure[58], a plot of ln($k_0$) vs. ln($\eta$) is predicted to be linear, with a slope of –θ, as shown in Figure 4b. Evidently, ln($k_0$) and ln($\eta$) are linearly related ($r^2$ = 0.97), with a slope of -1.0 and an intercept of -5.4 obtained by linear regression of the experimental data. The value of θ obtained from the slope, 1.0, indicates that the $Fc^{0/+}$ process is adiabatic and that $\Delta G_{os}^{\ddagger}$ makes a dominant contribution to $\Delta G^{\ddagger}$

(*i.e.*, solvent relaxation dynamics control the electron transfer rate). The linear relationship also implies that the influence of ion-pairing and/or double layer effects on the measured $k^0$ values is negligible or at least relatively invariant with respect to IL structure.

From Figure 4b, it is also evident that the $k^0$ value associated with the $Fc^{0/+}$ process shows a slight dependence on the constituent anion of the IL, with the $[NTf_2]^-$ ILs (red data points) generally lying much closer to the linear regression line ($r^2$ = 0.99 when only considering the $[NTf_2]^-$ ILs) compared to the non-$[NTf_2]^-$ ILs (blue data points). Given that $Fc^+$ is a positively charged species, the slight anion dependence of the $Fc^{0/+}$ process is not surprising, and this thought to arise due to slight changes in $\Delta G_{os}^{\ddagger}$ with different constituent anions (see Eq. 11). This is consistent with the fact that although the $Fc^{0/+}$ process is often quoted as possessing thermodynamic properties which are 'independent of the nature of the solvent', many studies have highlighted that this is unlikely to be the case.[11, 60] Finally, extrapolating the plot shown in Figure 4b to $\eta$ = 0.48 cP, which is the viscosity of an acetonitrile solution containing 0.3 M $[NBu_4][ClO_4]$ at 22°C, gives a $k^0$ value of approximately 10 cm $s^{-1}$, which again, is consistent with the value measured by Sun and Mirkin (8.4 ± 0.2 cm $s^{-1}$ and 8 ± 1 cm $s^{-1}$ on platinum and gold nanoelectrodes, respectively) under these conditions.[10, 61]

As noted above, and discussed in detail in our previous study[27], under a given set of conditions with FTAC voltammetry, the electron transfer kinetics of the $Fc^{0/+}$ process become further removed from reversible as the viscosity of the medium is increased. This is because while $k^0$ scales linearly with $\eta^{-1}$ (see Figure 4b), the upper limit of detection for $k^0$ is governed by the rate of mass-transport, which, under the transient conditions of FTAC voltammetry, means proportional to $D^{1/2}$ (or $\eta^{-1/2}$, see Eq. 8). As a result, as viscosity is increased, the kinetics of a given process decrease at a faster rate than the upper limit of detection, and this is why only a single, low frequency (9 or 37 Hz) was required to quantify $k^0$ ($Fc^{0/+}$) in the most viscous ILs shown in Table 3.

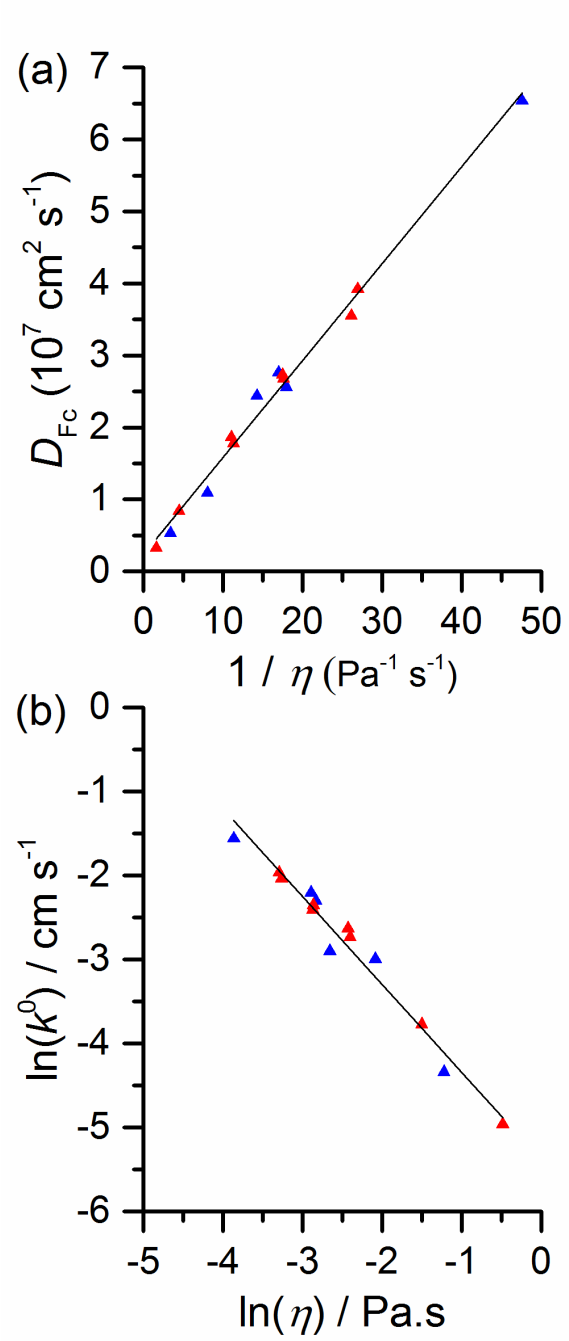


**Figure 4.** Plots of (a) $D_{Fc}$ vs. 1/ $\eta$ and (b) ln($k^0$) vs. ln($\eta$). Shown on the plots are lines of best fit obtained by linear regression of the data, with $r^2$ values of 0.99 and 0.97 in (a) and (b), respectively. In the plots, $[NTf_2]^-$ and non-$[NTf_2]^-$ ILs are represented by red and blue triangles, respectively.

## Conclusions

The mass-transport and heterogeneous electron-transfer kinetics associated with the $Fc^{0/+}$ process has been investigated in 14 non-haloaluminate ILs with dynamic viscosities ($\eta$) ranging from 20 to 620 cP. The $Fc^{0/+}$ process was simulated under DC cyclic voltammetric conditions at a 50 μm diameter platinum microdisk with a scan rate of 50 mV $s^{-1}$ and was found to be electrochemically reversible on this timescale. $D_{Fc}$ was calculated using convolution voltammetry and was found to be inversely proportional to the viscosity of the medium (*i.e.*, $D \propto 1/\eta$), as per the Stokes-Einstein relation. Analysis of the $D_{Fc}$ vs. $1/\eta$ data suggests that the mass-transport of Fc approaches 'perfect slip' behaviour in IL media. $k^0$ was measured using FTAC voltammetry, and a plot of $\ln(k^0)$ vs. $\ln(\eta)$ was found to be linear, with a slope of -1.0, which, in accordance with the Marcus theory of electron transfer, suggests that the $Fc^{0/+}$ process is adiabatic and that $\Delta G_{os}^{\ddagger}$ makes a dominant contribution to $\Delta G^{\ddagger}$. Analysis of the $\ln(k^0)$ vs. $\ln(\eta)$ data revealed a slight dependence of $k^0$ on the constituent anion of the IL, which was attributed to electrostatic interactions between the anion and positively charged $Fc^+$. Finally, by extrapolating the $D$ vs. $1/\eta$ and $\ln(k^0)$ vs. $\ln(\eta)$ plots to $\eta$ values typically encountered in acetonitrile-based electrolyte media, $D$ and $k^0$ values of approximately $2 \times 10^{-5}$ $cm^2$ $s^{-1}$ and 10 cm $s^{-1}$ were predicted, in excellent agreement with the studies by Mirkin and co-workers. Overall, the results indicate that the $Fc^{0/+}$ redox couple displays the characteristics of an "ideal" outer-sphere electron transfer process in IL media. In a more general sense, the results also highlight the advantages of convolution voltammetry and FTAC voltammetry, for quantifying mass-transport and electrode kinetics, respectively, in IL media.

## Associated Content

**Supporting information.** FTAC voltammograms obtained from the $Fc^{0/+}$ process in a range of ILs (Figures S1 to S31).

## Author Information


### Corresponding Authors

Alan.Bond@monash.edu (A.M.B.), +61 3 9905 1338

Jie.Zhang@monash.edu (J.Z.), +61 3 9905 6289


### Notes

The authors declare no competing financial interest.

## Acknowledgements


Financial support of this project from the Australian Research Council is gratefully acknowledged.

## References


1. Bard, A. J.; Faulkner, L. R., *Electrochemical Methods : Fundamentals and Applications*, 2nd ed.; Wiley: New York, 2001.

2. Mirkin, M. V., 15 - Determination of Electrode Kinetics. In *Handbook of Electrochemistry*, Zoski, C. G., Ed. Elsevier: Amsterdam, 2007; pp 639-660.

3. Rubinstein, I., *Physical Electrochemistry : Principles, Methods, and Applications*; M. Dekker: New York, 1995.

4. Marcus, R. A., Chemical + Electrochemical Electron-Transfer Theory. *Annu. Rev. Phys. Chem.* **1964**, *15*, 155-196.

5. Wilkes, J. S., A Short History of Ionic Liquids - from Molten Salts to Neoteric Solvents. *Green Chem.* **2002**, *4*, 73-80.

6. Galinski, M.; Lewandowski, A.; Stepniak, I., Ionic Liquids as Electrolytes. *Electrochim. Acta* **2006**, *51*, 5567-5580.

7. Armand, M.; Endres, F.; MacFarlane, D. R.; Ohno, H.; Scrosati, B., Ionic-Liquid Materials for the Electrochemical Challenges of the Future. *Nat. Mater.* **2009**, *8*, 621-629.

8. Bentley, C. L.; Bond, A. M.; Hollenkamp, A. F.; Mahon, P. J.; Zhang, J., Voltammetric Determination of the Iodide/Iodine Formal Potential and Triiodide Stability Constant in Conventional and Ionic Liquid Media. *J. Phys. Chem. C* **2015**, *119*, 22392-22403.

9. Nicholson, R. S., Theory and Application of Cyclic Voltammetry for Measurement of Electrode Reaction Kinetics. *Anal. Chem.* **1965**, *37*, 1351-1355.

10. Sun, P.; Mirkin, M. V., Kinetics of Electron-Transfer Reactions at Nanoelectrodes. *Anal. Chem.* **2006**, *78*, 6526-6534.

11. Bond, A. M.; McLennan, E. A.; Stojanovic, R. S.; Thomas, F. G., Assessment of Conditions under Which the Oxidation of Ferrocene Can Be Used as a Standard Voltammetric Reference Process in Aqueous Media. *Anal. Chem.* **1987**, *59*, 2853-2860.

12. Stojanovic, R. S.; Bond, A. M., Examination of Conditions under Which the Reduction of the Cobaltocenium Cation Can Be Used as a Standard Voltammetric Reference Process in Organic and Aqueous Solvents. *Anal. Chem.* **1993**, *65*, 56-64.

13. Gritzner, G.; Kuta, J., Recommendations on Reporting Electrode-Potentials in Nonaqueous Solvents. *Pure Appl. Chem.* **1984**, *56*, 461-466.

14. Fawcett, W. R.; Opallo, M., The Kinetics of Heterogeneous Electron Transfer Reaction in Polar Solvents. *Angew. Chem., Int. Ed. Engl.* **1994**, *33*, 2131-2143.

15. Eisele, S.; Schwarz, M.; Speiser, B.; Tittel, C., Diffusion Coefficient of Ferrocene in 1-Butyl-3-Methylimidazolium Tetrafluoroborate - Concentration Dependence and Solvent Purity. *Electrochim. Acta* **2006**, *51*, 5304-5306.

16. Nagy, L.; Gyetvai, G.; Kollar, L.; Nagy, G., Electrochemical Behavior of Ferrocene in Ionic Liquid Media. *J. Biochem. Biophys. Methods* **2006**, *69*, 121-132.

17. Fietkau, N.; Clegg, A. D.; Evans, R. G.; Villagrán, C.; Hardacre, C.; Compton, R. G., Electrochemical Rate Constants in Room Temperature Ionic Liquids: The Oxidation of a Series of Ferrocene Derivatives. *ChemPhysChem* **2006**, *7*, 1041-1045.

18. Rogers, E. I.; Silvester, D. S.; Poole, D. L.; Aldous, L.; Hardacre, C.; Compton, R. G., Voltammetric Characterization of the Ferrocene|Ferrocenium and Cobaltocenium|Cobaltocene Redox Couples in RTILs. *J. Phys. Chem. C* **2008**, *112*, 2729-2735.

19. Tachikawa, N.; Katayama, Y.; Miura, T., Electrode Kinetics of Ferrocenium/Ferrocene in Room-Temperature Ionic Liquids. *ECS Trans.* **2009**, *16*, 589-595.

20. Lovelock, K. R. J.; Cowling, F. N.; Taylor, A. W.; Licence, P.; Walsh, D. A., Effect of Viscosity on Steady-State Voltammetry and Scanning Electrochemical Microscopy in Room Temperature Ionic Liquids. *J. Phys. Chem. B* **2010**, *114*, 4442-4450.

21. Pan, Y. F.; Cleland, W. E.; Hussey, C. L., Heterogeneous Electron Transfer Kinetics and Diffusion of Ferrocene/Ferrocenium in Bis(Trifluoromethylsulfonyl)Imide-Based Ionic Liquids. *J. Electrochem. Soc.* **2012**, *159*, F125-F133.

22. Atkins, P. W.; De Paula, J., *Atkins' Physical Chemistry*, 9th ed.; Oxford University Press: Oxford, 2010.

23. Brooks, C. A.; Doherty, A. P., Concentration-Dependent Diffusion in Room Temperature Ionic Liquids: A Microelectrode Study. *Electrochem. Commun.* **2004**, *6*, 867-871.

24. Barnes, A. S.; Rogers, E. I.; Streeter, I.; Aldous, L.; Hardacre, C.; Compton, R. G., Extraction of Electrode Kinetic Parameters from Microdisc Voltammetric Data Measured under Transport Conditions Intermediate between Steady-State Convergent and Transient Linear Diffusion as Typically Applies to Room Temperature Ionic Liquids. *J. Phys. Chem. B* **2008**, *112*, 7560-7565.

25. Fontaine, O.; Lagrost, C.; Ghilane, J.; Martin, P.; Trippe, G.; Fave, C.; Lacroix, J. C.; Hapiot, P.; Randriamahazaka, H. N., Mass Transport and Heterogeneous Electron Transfer of

a Ferrocene Derivative in a Room-Temperature Ionic Liquid. *J. Electroanal. Chem.* **2009**, *632*, 88-96.

26. Lagrost, C.; Carrié, D.; Vaultier, M.; Hapiot, P., Reactivities of Some Electrogenerated Organic Cation Radicals in Room-Temperature Ionic Liquids: Toward an Alternative to Volatile Organic Solvents? *J. Phys. Chem. A* **2003**, *107*, 745-752.

27. Li, J.; Bentley, C. L.; Bond, A. M.; Zhang, J., Dual-Frequency Alternating Current Designer Waveform for Reliable Voltammetric Determination of Electrode Kinetics Approaching the Reversible Limit. *Anal. Chem.* **2016**, *88*, 2367-2374.

28. Bentley, C. L.; Bond, A. M.; Hollenkamp, A. F.; Mahon, P. J.; Zhang, J., Applications of Convolution Voltammetry in Electroanalytical Chemistry. *Anal. Chem.* **2014**, *86*, 2073–2081.

29. Bond, A. M.; Elton, D.; Guo, S. X.; Kennedy, G. F.; Mashkina, E.; Simonov, A. N.; Zhang, J., An Integrated Instrumental and Theoretical Approach to Quantitative Electrode Kinetic Studies Based on Large Amplitude Fourier Transformed A.C. Voltammetry: A Mini Review. *Electrochem. Commun.* **2015**, *57*, 78-83.

30. Bond, A. M.; Duffy, N. W.; Guo, S.-X.; Zhang, J.; Elton, D., Changing the Look of Voltammetry. *Anal. Chem.* **2005**, *77*, 186 A-195 A.

31. Wightman, R. M.; Wipf, D. O., *In Electroanalytical Chemistry*; Marcel Dekker: New York, 1989; Vol. 15.

32. Mahon, P. J.; Oldham, K. B., Convolutive Modelling of Electrochemical Processes Based on the Relationship between the Current and the Surface Concentration. *J. Electroanal. Chem.* **1999**, *464*, 1-13.

33. Zhang, J.; Guo, S.-X.; Bond, A. M., Discrimination and Evaluation of the Effects of Uncompensated Resistance and Slow Electrode Kinetics from the Higher Harmonic Components of a Fourier Transformed Large-Amplitude Alternating Current Voltammogram. *Anal. Chem.* **2007**, *79*, 2276-2288.

34. Feldberg, S. W., Optimization of Explicit Finite-Difference Simulation of Electrochemical Phenomena Utilizing an Exponentially Expanded Space Grid: Refinement of the Joslin-Pletcher Algorithm. *J. Electroanal. Chem.* **1981**, *127*, 1-10.

35. Rudolph, M., A Fast Implicit Finite Difference Algorithm for the Digital Simulation of Electrochemical Processes. *J. Electroanal. Chem.* **1991**, *314*, 13-22.

36. Zhang, J.; Guo, S.-X.; Bond, A. M.; Marken, F., Large-Amplitude Fourier Transformed High-Harmonic Alternating Current Cyclic Voltammetry: Kinetic Discrimination of Interfering Faradaic Processes at Glassy Carbon and at Boron-Doped Diamond Electrodes. *Anal. Chem.* **2004**, *76*, 3619-3629.

37. Sher, A. A.; Bond, A. M.; Gavaghan, D. J.; Harriman, K.; Feldberg, S. W.; Duffy, N. W.; Guo, S.-X.; Zhang, J., Resistance, Capacitance, and Electrode Kinetic Effects in Fourier-Transformed Large-Amplitude Sinusoidal Voltammetry: Emergence of Powerful and Intuitively Obvious Tools for Recognition of Patterns of Behavior. *Anal. Chem.* **2004**, *76*, 6214-6228.

38. Bond, A. M.; Duffy, N. W.; Elton, D. M.; Fleming, B. D., Characterization of Nonlinear Background Components in Voltammetry by Use of Large Amplitude Periodic Perturbations and Fourier Transform Analysis. *Anal. Chem.* **2009**, *81*, 8801-8808.

39. Bentley, C. L.; Bond, A. M.; Hollenkamp, A. F.; Mahon, P. J.; Zhang, J., Mass Transport Studies and Hydrogen Evolution at a Platinum Electrode Using

Bis(Trifluoromethanesulfonyl)Imide as the Proton Source in Ionic Liquids and Conventional Solvents. *J. Phys. Chem. C* **2014**, *118*, 22439–22449.

40. Sukardi, S. K.; Zhang, J.; Burgar, I.; Horne, M. D.; Hollenkamp, A. F.; MacFarlane, D. R.; Bond, A. M., Prospects for a Widely Applicable Reference Potential Scale in Ionic Liquids Based on Ideal Reversible Reduction of the Cobaltocenium Cation. *Electrochem. Commun.* **2008**, *10*, 250-254.

41. Evans, R. G.; Klymenko, O. V.; Hardacre, C.; Seddon, K. R.; Compton, R. G., Oxidation of N,N,N′,N′-Tetraalkyl-Para-Phenylenediamines in a Series of Room Temperature Ionic Liquids Incorporating the Bis(Trifluoromethylsulfonyl)Imide Anion. *J. Electroanal. Chem.* **2003**, *556*, 179-188.

42. Ue, M., Mobility and Ionic Association of Lithium and Quaternary Ammonium Salts in Propylene Carbonate and Γ-Butyrolactone. *J. Electrochem. Soc.* **1994**, *141*, 3336-3342.

43. Robinson, R. A.; Stokes, R. H., *Electrolyte Solutions. The Measurement and Interpretation of Conductance, Chemical Potential and Diffusion in Solutions of Simple Electrolytes.*, 2nd ed.; Butterworths Scientific Publications: London, 1959.

44. Matsuura, N.; Umemoto, K.; Takeda, Y., Formulation of Stokes Radii in DMF, DMSO and Propylene Carbonate with Solvent Structure Cavity Size as Parameter. *Bull. Chem. Soc. Jpn.* **1975**, *48*, 2253-2257.

45. Edward, J. T., Molecular Volumes and Stokes-Einstein Equation. *J. Chem. Educ.* **1970**, *47*, 261-270.

46. Cussler, E. L., *Diffusion: Mass Transfer in Fluid Systems*, 3rd ed.; Cambridge University Press: New York, 2009.

47. Tokuda, H.; Hayamizu, K.; Ishii, K.; Susan, M. A. B. H.; Watanabe, M., Physicochemical Properties and Structures of Room Temperature Ionic Liquids. 2. Variation of Alkyl Chain Length in Imidazolium Cation. *J. Phys. Chem. B* **2005**, *109*, 6103-6110.

48. Hapiot, P.; Lagrost, C., Electrochemical Reactivity in Room-Temperature Ionic Liquids. *Chem. Rev.* **2008**, *108*, 2238-2264.

49. Bond, A. M.; Colton, R.; Harvey, J.; Hutton, R. S., Voltammetric Studies of Ferrocene and the Mercury Dithiophosphate System at Mercury Electrodes over a Temperature Range Encompassing the Mercury Liquid-Solid State Transition. *J. Electroanal. Chem.* **1997**, *426*, 145-155.

50. Takusagawa, F.; Koetzle, T. F., Neutron-Diffraction Study of the Crystal-Structure of Ferrocene. *Acta Crystallogr. Sect. B-Struct. Commun.* **1979**, *35*, 1074-1081.

51. Tsierkezos, N. G., Cyclic Voltammetric Studies of Ferrocene in Nonaqueous Solvents in the Temperature Range from 248.15 to 298.15 K. *J. Solution Chem.* **2007**, *36*, 289-302.

52. Pyati, R.; Murray, R. W., Solvent Dynamics Effects on Heterogeneous Electron Transfer Rate Constants of Cobalt Tris(Bipyridine). *J. Am. Chem. Soc.* **1996**, *118*, 1743-1749.

53. Miao, W.; Ding, Z.; Bard, A. J., Solution Viscosity Effects on the Heterogeneous Electron Transfer Kinetics of Ferrocenemethanol in Dimethyl Sulfoxide−Water Mixtures. *J. Phys. Chem. B* **2002**, *106*, 1392-1398.

54. Zhang, X.; Leddy, J.; Bard, A. J., Dependence of Rate Constants of Heterogeneous Electron-Transfer Reactions on Viscosity. *J. Am. Chem. Soc.* **1985**, *107*, 3719-3721.

55. Williams, M. E.; Crooker, J. C.; Pyati, R.; Lyons, L. J.; Murray, R. W., A 10(11)-Fold Range of Solvent Dynamics Control of Heterogeneous Electron Transfers of Cobalt(III/II)-Tris(Bipyridine). *J. Am. Chem. Soc.* **1997**, *119*, 10249-10250.

56. Moressi, M. B.; Zón, M. A.; Fernández, H., Solvent Effects on the Heterogeneous Kinetics of N,N,N′,N′-Tetramethyl P-Phenylendiamine (TMPD) in Nonaqueous Binary Solvent Mixtures. The Role of the Preferential Solvation Phenomenon. *Electrochim. Acta* **2000**, *45*, 1669-1682.

57. Grampp, G.; Harrer, W.; Jaenicke, W., The Role of Solvent Reorganization Dynamics in Homogeneous Electron Self-Exchange Reactions. *J. Chem. Soc., Faraday Trans.* **1987**, *83*, 161-166.

58. Nakamura, K.; Shikata, T., Systematic Dielectric and NMR Study of the Ionic Liquid 1-Alkyl-3-Methyl Imidazolium. *ChemPhysChem* **2010**, *11*, 285-294.

59. Fawcett, W. R.; Gaal, A.; Misicak, D., Estimation of the Rate Constant for Electron Transfer in Room Temperature Ionic Liquids. *J. Electroanal. Chem.* **2011**, *660*, 230-233.

60. Noviandri, I.; Brown, K. N.; Fleming, D. S.; Gulyas, P. T.; Lay, P. A.; Masters, A. F.; Phillips, L., The Decamethylferrocenium/Decamethylferrocene Redox Couple: A Superior Redox Standard to the Ferrocenium/Ferrocene Redox Couple for Studying Solvent Effects on the Thermodynamics of Electron Transfer. *J. Phys. Chem. B* **1999**, *103*, 6713-6722.

61. Velmurugan, J.; Sun, P.; Mirkin, M. V., Scanning Electrochemical Microscopy with Gold Nanotips: The Effect of Electrode Material on Electron Transfer Rates. *J. Phys. Chem. C* **2009**, *113*, 459-464.

# For TOC Only:

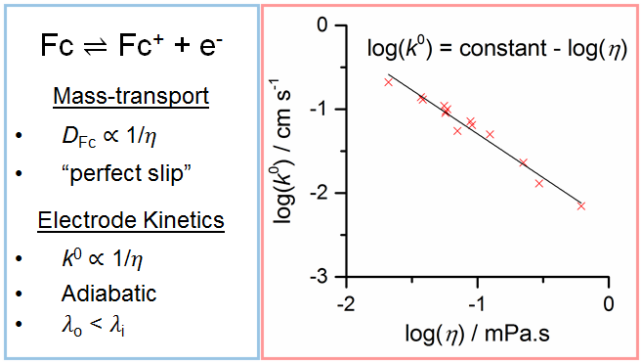
Fc ⇌ Fc+ + e-
Mass-transport
• $D_{Fc} \propto 1/\eta$
• "perfect slip"
Electrode Kinetics
• $k^0 \propto 1/\eta$
• Adiabatic
• $\lambda_o < \lambda_i$
log($k^0$) = constant - log($\eta$)
log($k^0$) / cm s$^{-1}$
0
-1
-2
-3
-2
-1
0
log($\eta$) / mPa.s